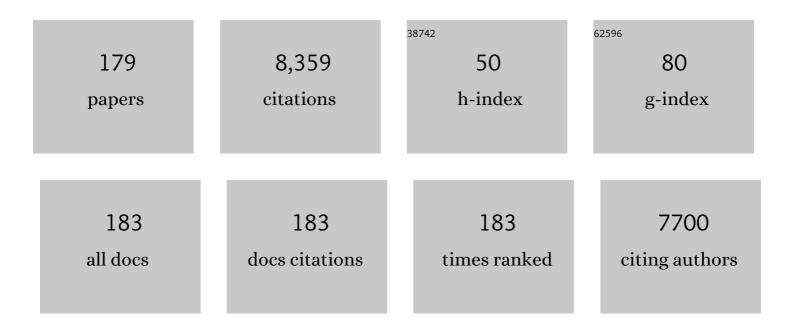
List of Publications by Year in descending order

Source: https://exaly.com/author-pdf/298531/publications.pdf Version: 2024-02-01



#	Article	IF	CITATIONS
1	Comprehensive biocompatible hemp fibers improved by phosphate zwitterion with high U(VI) affinity in the marine conditions. Chemical Engineering Journal, 2022, 430, 132742.	12.7	19
2	Constructing three-dimensional network C, O Co-doped nitrogen-deficient carbon nitride regulated by acrylic fluoroboron overall marine antifouling. Journal of Colloid and Interface Science, 2022, 608, 1802-1812.	9.4	1
3	Ultra-high flexibility amidoximated ethylene acrylic acid copolymer film synthesized by the mixed melting method for uranium adsorption from simulated seawater. Journal of Hazardous Materials, 2022, 426, 127808.	12.4	20
4	Constructing an Amino-reinforced amidoxime swelling layer on a Polyacrylonitrile surface for enhanced uranium adsorption from seawater. Journal of Colloid and Interface Science, 2022, 610, 1015-1026.	9.4	25
5	MOF-derived electrochemical catalyst Cu–N/C for the enhancement of amperometric oxygen detection. Nanoscale, 2022, 14, 1796-1806.	5.6	8
6	Synergistically Improved Antifouling Efficiency of a Bioinspired Self-renewing Interface via a Borneol/ Boron Acrylate Polymer. Journal of Colloid and Interface Science, 2022, 612, 459-466.	9.4	11
7	HFIP-functionalized 3D carbon nanostructure as chemiresistive nerve agents sensors under visible light. Sensors and Actuators B: Chemical, 2022, 358, 131475.	7.8	7
8	Mussel-inspired polydopamine microspheres self-adhered on natural hemp fibers for marine uranium harvesting and photothermal-enhanced antifouling properties. Journal of Colloid and Interface Science, 2022, 622, 109-116.	9.4	12
9	Eco-friendly silane as corrosion inhibitor for dual self-healing anticorrosion coatings. Journal of Coatings Technology Research, 2022, 19, 1381-1391.	2.5	3
10	Surface morphology properties and antifouling activity of Bi2WO6/boron-grafted polyurethane composite coatings realized via multiple synergy. Journal of Colloid and Interface Science, 2022, 626, 815-823.	9.4	7
11	Secretion mechanism and adhesive mechanism of diatoms: Direct evidence from the quantitative analysis. Micron, 2021, 140, 102951.	2.2	6
12	Photocatalytic antifouling coating based on carbon nitride with dynamic acrylate boron fluorinated polymers. New Journal of Chemistry, 2021, 45, 780-787.	2.8	5
13	Construction of Bi/Bi ₅ O ₇ I anchored on a polymer with boosted interfacial charge transfer for biofouling resistance and photocatalytic H ₂ evolution. Catalysis Science and Technology, 2021, 11, 1330-1336.	4.1	3
14	Zwitterionic modified electrostatic flocking surfaces for diatoms and mussels resistance. Journal of Colloid and Interface Science, 2021, 588, 9-18.	9.4	13
15	Swollen-layer constructed with polyamine on the surface of nano-polyacrylonitrile cloth used for extract uranium from seawater. Chemosphere, 2021, 271, 129548.	8.2	24
16	In situ construction of 3-dimensional hierarchical carbon nanostructure; investigation of the synthesis parameters and hydrogen evolution reaction performance. Carbon, 2021, 178, 48-57.	10.3	14
17	Bioinspired Durable Antibacterial and Antifouling Coatings Based on Borneol Fluorinated Polymers: Demonstrating Direct Evidence of Antiadhesion. ACS Applied Materials & Interfaces, 2021, 13, 33417-33426.	8.0	44
18	Slippery-Liquid-Infused Electrostatic Flocking Surfaces for Marine Antifouling Application. Langmuir, 2021, 37, 10020-10028.	3.5	9

#	Article	IF	CITATIONS
19	αâ^'Fe2O3/rGO cooperated with tri-alkyl-substituted-imidazolium ionic liquids for enhancing oxygen sensing. Sensors and Actuators B: Chemical, 2021, 341, 130029.	7.8	3
20	Surface hybridization of π-conjugate structure cyclized polyacrylonitrile and radial microsphere shaped TiO2 for reducing U(VI) to U(IV). Journal of Hazardous Materials, 2021, 416, 125812.	12.4	49
21	Binder-free metal-organic frameworks-derived CoP/Mo-doped NiCoP nanoplates for high-performance quasi-solid-state supercapacitors. Electrochimica Acta, 2021, 390, 138840.	5.2	17
22	Anti-bacterial and super-hydrophilic bamboo charcoal with amidoxime modified for efficient and selective uranium extraction from seawater. Journal of Colloid and Interface Science, 2021, 598, 455-463.	9.4	55
23	Ultra-high mechanical property and multi-layer porous structure of amidoximation ethylene-acrylic acid copolymer balls for efficient and selective uranium adsorption from radioactive wastewater. Chemosphere, 2021, 280, 130722.	8.2	21
24	Anti-corrosion coatings with active and passive protective performances based on v-COF/GO nanocontainers. Progress in Organic Coatings, 2021, 159, 106415.	3.9	5
25	The mussel-inspired micro-nano structure for antifouling:A flowering tree. Journal of Colloid and Interface Science, 2021, 603, 307-318.	9.4	12
26	Simple one-step synthesis of woven amidoximated natural material bamboo strips for uranium extraction from seawater. Chemical Engineering Journal, 2021, 425, 131538.	12.7	37
27	Corrosion protection coatings embedded with silane-functionalized rGO/SiO2 nanocontainers: Enhancing dispersive and corrosion-inhibitor loading capabilities. Surface and Coatings Technology, 2021, 427, 127850.	4.8	10
28	Crawling and adhesion behavior of Halamphora sp. based on different parts of Folium Sennae-like film: Evaluation of analytical methods for anti-diatom experimental results. Micron, 2021, 152, 103178.	2.2	0
29	Fabrication of the pod-like KCC-1/TiO2 superhydrophobic surface on AZ31 Mg alloy with stability and photocatalytic property. Applied Surface Science, 2020, 499, 143933.	6.1	23
30	A novel 3D reticular anti-fouling bio-adsorbent for uranium extraction from seawater: Polyethylenimine and guanidyl functionalized hemp fibers. Chemical Engineering Journal, 2020, 382, 122555.	12.7	82
31	A chitosan-graphene oxide/ZIF foam with anti-biofouling ability for uranium recovery from seawater. Chemical Engineering Journal, 2020, 382, 122850.	12.7	117
32	Mussel-inspired anti-biofouling and robust hybrid nanocomposite hydrogel for uranium extraction from seawater. Journal of Hazardous Materials, 2020, 381, 120984.	12.4	67
33	lonic liquid combined with NiCo2O4/rGO enhances electrochemical oxygen sensing. Talanta, 2020, 209, 120515.	5.5	15
34	Superhydrophobic nanoporous polymer-modified sponge for in situ oil/water separation. Chemosphere, 2020, 239, 124793.	8.2	29
35	Three-dimensional flower-like shaped Bi5O7I particles incorporation zwitterionic fluorinated polymers with synergistic hydration-photocatalytic for enhanced marine antifouling performance. Journal of Hazardous Materials, 2020, 389, 121854.	12.4	32
36	High efficiency biosorption of Uranium (VI) ions from solution by using hemp fibers functionalized with imidazole-4,5-dicarboxylic. Journal of Molecular Liquids, 2020, 297, 111739.	4.9	23

#	Article	IF	CITATIONS
37	Sandwich-like polyvinyl alcohol (PVA) grafted graphene: A solid-inhibitors container for long term self-healing coatings. Chemical Engineering Journal, 2020, 383, 123203.	12.7	36
38	Layer by layer inkjet printing reduced graphene oxide film supported nickel cobalt layered double hydroxide as a binder-free electrode for supercapacitors. Applied Surface Science, 2020, 509, 144872.	6.1	22
39	Fully Repairable Slippery Organogel Surfaces with Reconfigurable Paraffin-Based Framework for Universal Antiadhesion. ACS Applied Materials & Interfaces, 2020, 12, 39807-39816.	8.0	7
40	Facile synthesis of reduced graphene oxide encapsulated selenium nanoparticles prepared by hydrothermal method for acetone gas sensors. Chemical Physics Letters, 2020, 755, 137797.	2.6	21
41	Three-dimensional heterostructured polypyrrole/nickel molybdate anchored on carbon cloth for high-performance flexible supercapacitors. Journal of Colloid and Interface Science, 2020, 574, 355-363.	9.4	17
42	Anti-Biofouling and Water—Stable Balanced Charged Metal Organic Framework-Based Polyelectrolyte Hydrogels for Extracting Uranium from Seawater. ACS Applied Materials & Interfaces, 2020, 12, 18012-18022.	8.0	73
43	HFIP-functionalized electrospun WO3 hollow nanofibers/rGO as an efficient double layer sensing material for dimethyl methylphosphonate gas under UV-Light irradiation. Journal of Alloys and Compounds, 2020, 832, 154999.	5.5	23
44	Construction of gel-like swollen-layer on Polyacrylonitrile Surface and Its Swelling Behavior and Uranium Adsorption Properties. Journal of Colloid and Interface Science, 2020, 576, 109-118.	9.4	23
45	Preparation of a 3D multi-branched chelate adsorbent for high selective adsorption of uranium(VI): Acrylic and diaminomaleonitrile functionalized waste hemp fiber. Reactive and Functional Polymers, 2020, 149, 104512.	4.1	22
46	Ag-modified hexagonal nanoflakes-textured hollow octahedron Zn2SnO4 with enhanced sensing properties for triethylamine. Journal of Alloys and Compounds, 2020, 823, 153724.	5.5	17
47	Self-healing system adapted to different pH environments for active corrosion protection of magnesium alloy. Journal of Alloys and Compounds, 2020, 824, 153918.	5.5	32
48	Layer-by-Layer-Assembled antifouling films with surface microtopography inspired by Laminaria japonica. Applied Surface Science, 2020, 511, 145564.	6.1	36
49	Eco-friendly green synthesis of clove buds extract functionalized silver nanoparticles and evaluation of antibacterial and antidiatom activity. Journal of Microbiological Methods, 2020, 173, 105934.	1.6	54
50	Surface plasma Ag-decorated Bi5O7I microspheres uniformly distributed on a zwitterionic fluorinated polymer with superfunctional antifouling property. Applied Catalysis B: Environmental, 2020, 271, 118920.	20.2	46
51	Fabrication of electrospun Co3O4/CuO p-p heterojunctions nanotubes functionalized with HFIP for detecting chemical nerve agent under visible light irradiation. Sensors and Actuators B: Chemical, 2020, 314, 128076.	7.8	34
52	Ag-CS Enhanced Performance of Pyrrolidone-Based Ionic Liquid Oxygen Sensor. Journal of the Electrochemical Society, 2020, 167, 067522.	2.9	3
53	A hybrid sponge with guanidine and phytic acid enriched surface for integration of antibiofouling and uranium uptake from seawater. Applied Surface Science, 2020, 525, 146611.	6.1	18
54	In Situ Anchoring of Pyrrhotite on Graphitic Carbon Nitride Nanosheet for Efficient Immobilization of Uranium. Chemistry - A European Journal, 2019, 25, 590-597.	3.3	11

#	Article	IF	CITATIONS
55	Superaerophobic Quaternary Ni–Co–S–P Nanoparticles for Efficient Overall Water-Splitting. ACS Sustainable Chemistry and Engineering, 2019, 7, 14639-14646.	6.7	56
56	HFIPâ€Functionalized Co ₃ O ₄ Microâ€Nanoâ€Octahedra/rGO as a Doubleâ€Layer Sensing Material for Chemical Warfare Agents. Chemistry - A European Journal, 2019, 25, 11892-11902.	3.3	21
57	Layer-by-layer inkjet printing GO film and Ag nanoparticles supported nickel cobalt layered double hydroxide as a flexible and binder-free electrode for supercapacitors. Journal of Colloid and Interface Science, 2019, 557, 691-699.	9.4	41
58	Self-Adjusting Lubricant-Infused Porous Hydrophobic Sticky Surfaces: Programmable Time Delay Switch for Smart Control of the Drop's Slide. ACS Applied Materials & Interfaces, 2019, 11, 43681-43688.	8.0	4
59	Rationally designed CuCo2O4@Ni(OH)2 with 3D hierarchical core-shell structure for flexible energy storage. Journal of Colloid and Interface Science, 2019, 557, 76-83.	9.4	35
60	Design of 2D mesoporous Zn/Co-based metal-organic frameworks as a flexible electrode for energy storage and conversion. Journal of Power Sources, 2019, 438, 227057.	7.8	53
61	Heterogeneous NiSe ₂ /Ni Ultrafine Nanoparticles Embedded into an N,S-Codoped Carbon Framework for pH-Universal Hydrogen Evolution Reaction. ACS Sustainable Chemistry and Engineering, 2019, 7, 4119-4127.	6.7	29
62	Designed synthesis of Co-doped sponge-like In ₂ O ₃ for highly sensitive detection of acetone gas. CrystEngComm, 2019, 21, 1876-1885.	2.6	30
63	Fabrication of ZnO/epoxy resin superhydrophobic coating on AZ31 magnesium alloy. Chemical Engineering Journal, 2019, 368, 261-272.	12.7	150
64	Layer-by-layer inkjet printing GO film anchored Ni(OH)2 nanoflakes for high-performance supercapacitors. Chemical Engineering Journal, 2019, 375, 121988.	12.7	48
65	Longâ€Term Stability of a Liquidâ€Infused Coating with Antiâ€Corrosion and Antiâ€Icing Potentials on Al Alloy. ChemElectroChem, 2019, 6, 3911-3919.	3.4	16
66	Hyperbranched topological swollen-layer constructs of multi-active sites polyacrylonitrile (PAN) adsorbent for uranium(VI) extraction from seawater. Chemical Engineering Journal, 2019, 374, 1204-1213.	12.7	57
67	Carbon Cloth Modified with Metalâ€Organic Framework Derived CC@CoMoO ₄ o(OH) ₂ Nanosheets Array as a Flexible Energy‣torage Material. ChemElectroChem, 2019, 6, 3355-3366.	3.4	14
68	Magnetic metal-organic frameworks/carbon dots as a multifunctional platform for detection and removal of uranium. Applied Surface Science, 2019, 491, 640-649.	6.1	49
69	Nano-sized architectural design of multi-activity graphene oxide (GO) by chemical post-decoration for efficient uranium(VI) extraction. Journal of Hazardous Materials, 2019, 375, 320-329.	12.4	53
70	Grown Carbon Nanotubes on Electrospun Carbon Nanofibers as a 3D Carbon Nanomaterial for High Energy Storage Performance. ChemistrySelect, 2019, 4, 5437-5458.	1.5	15
71	Electrospun n-p WO3/CuO heterostructure nanofibers as an efficient sarin nerve agent sensing material at room temperature. Journal of Alloys and Compounds, 2019, 793, 31-41.	5.5	27
72	Designed synthesis of Ag-functionalized Ni-doped In ₂ O ₃ nanorods with enhanced formaldehyde gas sensing properties. Journal of Materials Chemistry C, 2019, 7, 7219-7229.	5.5	49

#	Article	IF	CITATIONS
73	3D Cu(OH)2 nanowires/carbon cloth for flexible supercapacitors with outstanding cycle stability. Chemical Engineering Journal, 2019, 371, 348-355.	12.7	59
74	Graphene Oxide and Silver Ions Coassisted Zeolitic Imidazolate Framework for Antifouling and Uranium Enrichment from Seawater. ACS Sustainable Chemistry and Engineering, 2019, 7, 6185-6195.	6.7	73
75	Self-healing liquid-infused surfaces with high transparency for optical devices. MRS Communications, 2019, 9, 92-98.	1.8	12
76	Fabrication of uniform 1-D ZnO/ZnCo2O4 nano-composite and enhanced properties in gas sensing detection. Materials Chemistry and Physics, 2019, 228, 66-74.	4.0	17
77	Outstanding cavitation erosion resistance of hydrophobic polydimethylsiloxaneâ€based polyurethane coatings. Journal of Applied Polymer Science, 2019, 136, 47668.	2.6	16
78	An anti-algae adsorbent for uranium extraction: l-Arginine functionalized graphene hydrogel loaded with Ag nanoparticles. Journal of Colloid and Interface Science, 2019, 543, 192-200.	9.4	27
79	Fast self-replenishing slippery surfaces with a 3D fibrous porous network for the healing of surface properties. Journal of Materials Chemistry A, 2019, 7, 24900-24907.	10.3	26
80	Mussel-inspired antifouling magnetic activated carbon for uranium recovery from simulated seawater. Journal of Colloid and Interface Science, 2019, 534, 172-182.	9.4	52
81	Defect-Induced Method for Preparing Hierarchical Porous Zr–MOF Materials for Ultrafast and Large-Scale Extraction of Uranium from Modified Artificial Seawater. Industrial & Engineering Chemistry Research, 2019, 58, 1159-1166.	3.7	52
82	3D hybrid Ni-Multiwall carbon nanotubes/carbon nanofibers for detecting sarin nerve agent at room temperature. Journal of Alloys and Compounds, 2019, 780, 680-689.	5.5	33
83	Core-shell structure of ZnO/Co3O4 composites derived from bimetallic-organic frameworks with superior sensing performance for ethanol gas. Applied Surface Science, 2019, 475, 700-709.	6.1	101
84	Hierarchical NiSe@Co2(CO3)(OH)2 heterogeneous nanowire arrays on nickel foam as electrode with high areal capacitance for hybrid supercapacitors. Electrochimica Acta, 2019, 294, 325-336.	5.2	55
85	One-pot synthesis of cubic ZnSnO3/ZnO heterostructure composite and enhanced gas-sensing performance. Journal of Alloys and Compounds, 2019, 780, 193-201.	5.5	55
86	Highly efficient immobilization of uranium(VI) from aqueous solution by phosphonate-functionalized dendritic fibrous nanosilica (DFNS). Journal of Hazardous Materials, 2019, 363, 248-257.	12.4	88
87	The efficient immobilization of uranium(<scp>vi</scp>) by modified dendritic fibrous nanosilica (DFNS) using mussel bioglue. Inorganic Chemistry Frontiers, 2019, 6, 746-755.	6.0	12
88	Efficient removal of U(<scp>vi</scp>) from simulated seawater with hyperbranched polyethylenimine (HPEI) covalently modified SiO ₂ coated magnetic microspheres. Inorganic Chemistry Frontiers, 2018, 5, 1321-1328.	6.0	39
89	Functionalized Sugarcane Bagasse for U(VI) Adsorption from Acid and Alkaline Conditions. Scientific Reports, 2018, 8, 793.	3.3	21
90	Hierarchical metal-organic framework derived nitrogen-doped porous carbon by controllable synthesis for high performance supercapacitors. Journal of Electroanalytical Chemistry, 2018, 813, 200-207.	3.8	27

#	Article	IF	CITATIONS
91	Ni–Mn LDH-decorated 3D Fe-inserted and N-doped carbon framework composites for efficient uranium(<scp>vi</scp>) removal. Environmental Science: Nano, 2018, 5, 467-475.	4.3	77
92	Hierarchical NiCo2S4@CoMoO4 core-shell heterostructures nanowire arrays as advanced electrodes for flexible all-solid-state asymmetric supercapacitors. Applied Surface Science, 2018, 453, 73-82.	6.1	206
93	High efficiency extraction of U(VI) from seawater by incorporation of polyethyleneimine, polyacrylic acid hydrogel and Luffa cylindrical fibers. Chemical Engineering Journal, 2018, 345, 526-535.	12.7	71
94	Polyethyleneimine-functionalized Luffa cylindrica for efficient uranium extraction. Journal of Colloid and Interface Science, 2018, 530, 538-546.	9.4	35
95	Preparation of Ultrathin Chiffon-like Ni-Al LDHs/Graphene Composite: Interlayer Stacking of Two-Dimensional Charged Panels via Electrostatic Self-Assembly for Supercapacitor Electrodes. Journal of the Electrochemical Society, 2018, 165, A784-A792.	2.9	6
96	PtO 2 -nanoparticles functionalized CuO polyhedrons for n-butanol gas sensor application. Ceramics International, 2018, 44, 10426-10432.	4.8	56
97	Efficient extraction of uranium from aqueous solution using an amino-functionalized magnetic titanate nanotubes. Journal of Hazardous Materials, 2018, 353, 9-17.	12.4	74
98	Ionic liquids combined with Pt-modified ordered mesoporous carbons as electrolytes for the oxygen sensing. Sensors and Actuators B: Chemical, 2018, 254, 490-501.	7.8	10
99	Rapid and efficient uranium(VI) capture by phytic acid/polyaniline/FeOOH composites. Journal of Colloid and Interface Science, 2018, 511, 1-11.	9.4	54
100	Efficient removal of uranium(<scp>vi</scp>) from simulated seawater with hyperbranched polyethylenimine (HPEI)-functionalized polyacrylonitrile fibers. New Journal of Chemistry, 2018, 42, 168-176.	2.8	51
101	Hierarchical FeCo2O4@NiCo layered double hydroxide core/shell nanowires for high performance flexible all-solid-state asymmetric supercapacitors. Chemical Engineering Journal, 2018, 334, 1573-1583.	12.7	360
102	Effects of TiB ₂ /TiC <i>_x</i> ratios on compression properties and abrasive wear resistance of in situ 50â€vol% (TiB ₂ –TiC <i>_x</i>)/Al–Cu composites. Powder Metallurgy, 2018, 61, 81-87.	1.7	3
103	Electrochemical Oxygen Sensor Based on the Interaction of Double-Layer Ionic Liquid Film (DLILF). Journal of the Electrochemical Society, 2018, 165, B779-B786.	2.9	11
104	Electrochemical Mix-Reduction Process of U and U-Fe Alloys on the Surface of Cathode in LiCl-KCl-U3 O8 at 773â€K. ChemElectroChem, 2018, 5, 2697-2697.	3.4	1
105	Hierarchical FeCo ₂ O ₄ @polypyrrole Core/Shell Nanowires on Carbon Cloth for High-Performance Flexible All-Solid-State Asymmetric Supercapacitors. ACS Sustainable Chemistry and Engineering, 2018, 6, 14945-14954.	6.7	117
106	Hierarchical Ni–Al Layered Double Hydroxide In Situ Anchored onto Polyethylenimine-Functionalized Fibers for Efficient U(VI) Capture. ACS Sustainable Chemistry and Engineering, 2018, 6, 13385-13394.	6.7	45
107	RGO nanosheets modified NiCo2S4 nanoflowers for improved ethanol sensing performance at low temperature. Chemical Physics Letters, 2018, 703, 80-85.	2.6	9
108	Phosphatidyl-assisted fabrication of graphene oxide nanosheets with multiple active sites for uranium(vi) capture. Environmental Science: Nano, 2018, 5, 1584-1594.	4.3	18

#	Article	IF	CITATIONS
109	Investigation of uranium (VI) adsorption by poly(dopamine) functionalized waste paper derived carbon. Journal of the Taiwan Institute of Chemical Engineers, 2018, 91, 266-273.	5.3	31
110	A flexible all-solid-state asymmetric supercapacitors based on hierarchical carbon cloth@CoMoO4@NiCo layered double hydroxide core-shell heterostructures. Chemical Engineering Journal, 2018, 352, 29-38.	12.7	259
111	Novel Ion-Imprinted Carbon Material Induced by Hyperaccumulation Pathway for the Selective Capture of Uranium. ACS Applied Materials & amp; Interfaces, 2018, 10, 28877-28886.	8.0	45
112	Electrochemical Mixâ€Reduction Process of U and Uâ€Fe Alloys on the Surface of Cathode in LiClâ€KClâ€U ₃ O ₈ at 773â€K. ChemElectroChem, 2018, 5, 2738-2746.	3.4	7
113	Metallic and superhydrophilic nickel cobalt diselenide nanosheets electrodeposited on carbon cloth as a bifunctional electrocatalyst. Journal of Materials Chemistry A, 2018, 6, 17353-17360.	10.3	100
114	A novel U(<scp>vi</scp>)-imprinted graphitic carbon nitride composite for the selective and efficient removal of U(<scp>vi</scp>) from simulated seawater. Inorganic Chemistry Frontiers, 2018, 5, 2218-2226.	6.0	36
115	Polypyrrole modified Fe ⁰ -loaded graphene oxide for the enrichment of uranium(<scp>vi</scp>) from simulated seawater. Dalton Transactions, 2018, 47, 12984-12992.	3.3	20
116	Template-free synthesis of rGO decorated hollow Co3O4 nano/microspheres for ethanol gas sensor. Ceramics International, 2018, 44, 21091-21098.	4.8	48
117	Superhydrophilic phosphate and amide functionalized magnetic adsorbent: a new combination of anti-biofouling and uranium extraction from seawater. Environmental Science: Nano, 2018, 5, 2346-2356.	4.3	44
118	Removal U(VI) from artificial seawater using facilely and covalently grafted polyacrylonitrile fibers with lysine. Applied Surface Science, 2017, 403, 378-388.	6.1	64
119	Hierarchical Co 3 O 4 @Ni(OH) 2 core-shell nanosheet arrays for isolated all-solid state supercapacitor electrodes with superior electrochemical performance. Chemical Engineering Journal, 2017, 315, 35-45.	12.7	239
120	Preparation and characterization of ZnO/CoNiO2 hollow nanofibers by electrospinning method with enhanced gas sensing properties. Journal of Alloys and Compounds, 2017, 702, 20-30.	5.5	35
121	Tube in tube ZnO/ZnCo ₂ O ₄ nanostructure synthesized by facile single capillary electrospinning with enhanced ethanol gas-sensing properties. RSC Advances, 2017, 7, 11428-11438.	3.6	35
122	Fabrication of ZIF-8@SiO ₂ Micro/Nano Hierarchical Superhydrophobic Surface on AZ31 Magnesium Alloy with Impressive Corrosion Resistance and Abrasion Resistance. ACS Applied Materials & Interfaces, 2017, 9, 11106-11115.	8.0	219
123	Bovine Serum Albumin-Coated Graphene Oxide for Effective Adsorption of Uranium(VI) from Aqueous Solutions. Industrial & Engineering Chemistry Research, 2017, 56, 3588-3598.	3.7	75
124	Controllable synthesis and enhanced gas sensing properties of a single-crystalline WO ₃ –rGO porous nanocomposite. RSC Advances, 2017, 7, 14192-14199.	3.6	51
125	Hierarchically structured layered-double-hydroxides derived by ZIF-67 for uranium recovery from simulated seawater. Journal of Hazardous Materials, 2017, 338, 167-176.	12.4	125
126	High-performance all-solid-state asymmetrical supercapacitors based on petal-like NiCo 2 S 4 /Polyaniline nanosheets. Chemical Engineering Journal, 2017, 325, 134-143.	12.7	201

#	Article	IF	CITATIONS
127	Shape-controlled fabrication and enhanced gas sensing properties of uniform sphere-like ZnFe 2 O 4 hierarchical architectures. Sensors and Actuators B: Chemical, 2017, 250, 111-120.	7.8	54
128	Impact of addition sheet-like cobalt in ionic liquids mixture to detect oxygen. Talanta, 2017, 172, 182-185.	5.5	3
129	P–p heterojunction CuO/CuCo ₂ O ₄ nanotubes synthesized via electrospinning technology for detecting n-propanol gas at room temperature. Inorganic Chemistry Frontiers, 2017, 4, 1219-1230.	6.0	63
130	Effect of the synthesis method on the performance of Fe3O4–inositol hexaphosphate as a drug delivery vehicle for combination therapeutics with doxorubicin. New Journal of Chemistry, 2017, 41, 5305-5312.	2.8	8
131	Enhanced acetone gas sensing response of ZnO/ZnCo2O4 nanotubes synthesized by single capillary electrospinning technology. Sensors and Actuators B: Chemical, 2017, 252, 511-522.	7.8	47
132	Enhancing adsorption of U(VI) onto EDTA modified L. cylindrica using epichlorohydrin and ethylenediamine as a bridge. Scientific Reports, 2017, 7, 44156.	3.3	12
133	One‣tep Synthesis of Co ₃ O ₄ /Graphene Aerogels and Their All‣olid‣tate Asymmetric Supercapacitor. European Journal of Inorganic Chemistry, 2017, 2017, 1143-1152.	2.0	34
134	Rational Design of Sandwiched Ni–Co Layered Double Hydroxides Hollow Nanocages/Graphene Derived from Metal–Organic Framework for Sustainable Energy Storage. ACS Sustainable Chemistry and Engineering, 2017, 5, 9923-9934.	6.7	89
135	Hierarchical flower like double-layer superhydrophobic films fabricated on AZ31 for corrosion protection and self-cleaning. New Journal of Chemistry, 2017, 41, 12767-12776.	2.8	21
136	Efficient removal of uranium(<scp>vi</scp>) from simulated seawater using amidoximated polyacrylonitrile/FeOOH composites. Dalton Transactions, 2017, 46, 15746-15756.	3.3	44
137	Composites of hierarchical metal–organic framework derived nitrogen-doped porous carbon and interpenetrating 3D hollow carbon spheres from lotus pollen for high-performance supercapacitors. New Journal of Chemistry, 2017, 41, 12835-12842.	2.8	17
138	Water-repellent and corrosion-resistance properties of superhydrophobic and lubricant-infused super slippery surfaces. RSC Advances, 2017, 7, 44239-44246.	3.6	56
139	3D self-assembly polyethyleneimine modified graphene oxide hydrogel for the extraction of uranium from aqueous solution. Applied Surface Science, 2017, 426, 1063-1074.	6.1	69
140	Interfacial growth of a metal–organic framework (UiO-66) on functionalized graphene oxide (GO) as a suitable seawater adsorbent for extraction of uranium(<scp>vi</scp>). Journal of Materials Chemistry A, 2017, 5, 17933-17942.	10.3	253
141	\$\$extit{Ex},extit{situ}\$\$ Ex situ synthesis of G/ \$\$upalpha \$\$ α Bulletin of Materials Science, 2017, 40, 691-698.	1.7	15
142	Inâ€Situ Fabrication of MOFâ€Derived Coâ^'Co Layered Double Hydroxide Hollow Nanocages/Graphene Composite: A Novel Electrode Material with Superior Electrochemical Performance. Chemistry - A European Journal, 2017, 23, 14839-14847.	3.3	89
143	Co3O4 nanoparticle-decorated hierarchical flower-like α-Fe2O3 microspheres: Synthesis and ethanol sensing properties. Journal of Alloys and Compounds, 2017, 727, 52-62.	5.5	41
144	Melamine modified graphene hydrogels for the removal of uranium(<scp>vi</scp>) from aqueous solution. New Journal of Chemistry, 2017, 41, 10899-10907.	2.8	36

#	Article	IF	CITATIONS
145	Design of multifunctional phytate coated magnetic composites for combined therapy with antitumor drugs. New Journal of Chemistry, 2017, 41, 14898-14905.	2.8	0
146	Morphology controllable synthesis of NiCo 2 S 4 and application as gas sensors. Materials Letters, 2017, 188, 17-20.	2.6	16
147	Recovery of uranium(<scp>vi</scp>) from aqueous solutions using a modified honeycomb-like porous carbon material. Dalton Transactions, 2017, 46, 420-429.	3.3	68
148	Polypyrrole/cobalt ferrite/multiwalled carbon nanotubes as an adsorbent for removing uranium ions from aqueous solutions. Dalton Transactions, 2016, 45, 9166-9173.	3.3	31
149	Nickel-Cobalt Layered Double Hydroxide Nanowires on Three Dimensional Graphene Nickel Foam for High Performance Asymmetric Supercapacitors. Electrochimica Acta, 2016, 215, 492-499.	5.2	114
150	Combination therapeutics of doxorubicin with Fe ₃ O ₄ @chitosan@phytic acid nanoparticles for multi-responsive drug delivery. RSC Advances, 2016, 6, 88248-88254.	3.6	8
151	Catalytic effect of CuO nanoplates, a graphene (G)/CuO nanocomposite and an Al/G/CuO composite on the thermal decomposition of ammonium perchlorate. RSC Advances, 2016, 6, 74155-74161.	3.6	49
152	Application of Chemical Doping and Architectural Design Principles To Fabricate Nanowire Co ₂ Ni ₃ ZnO ₈ Arrays for Aqueous Asymmetric Supercapacitors. ACS Applied Materials & Interfaces, 2016, 8, 20157-20167.	8.0	16
153	Rational design of sandwich-like exfoliated nickel hydroxide–carbon nanotubes as a novel electrode for supercapacitors. RSC Advances, 2016, 6, 70999-71005.	3.6	4
154	Fabrication of CeO ₂ /ZnCo ₂ O ₄ n–p heterostructured porous nanotubes via electrospinning technology for enhanced ethanol gas sensing performance. RSC Advances, 2016, 6, 101626-101637.	3.6	24
155	Porous tungsten trioxide nanolamellae with uniform structures for high-performance ethanol sensing. CrystEngComm, 2016, 18, 8411-8418.	2.6	25
156	Three-dimensional hierarchical Co ₃ O ₄ nano/micro-architecture: synthesis and ethanol sensing properties. CrystEngComm, 2016, 18, 5728-5735.	2.6	29
157	Synthesis of ketoxime-functionalized Fe ₃ O ₄ @C core–shell magnetic microspheres for enhanced uranium(<scp>vi</scp>) removal. RSC Advances, 2016, 6, 22179-22186.	3.6	21
158	In situ growth of ZnO nanorod arrays on cotton cloth for the removal of uranium(<scp>vi</scp>). RSC Advances, 2015, 5, 53433-53440.	3.6	15
159	Synthesis of exfoliated titanium dioxide nanosheets/nickel–aluminum layered double hydroxide as a novel electrode for supercapacitors. RSC Advances, 2015, 5, 49204-49210.	3.6	10
160	Mesoporous V ₂ O ₅ /Ketjin black nanocomposites for all-solid-state symmetric supercapacitors. CrystEngComm, 2015, 17, 1673-1679.	2.6	27
161	Fabrication of super slippery sheet-layered and porous anodic aluminium oxide surfaces and its anticorrosion property. Applied Surface Science, 2015, 355, 495-501.	6.1	72
162	The growth and assembly of the multidimensional hierarchical Ni ₃ S ₂ for aqueous asymmetric supercapacitors. CrystEngComm, 2015, 17, 4495-4501.	2.6	44

#	Article	IF	CITATIONS
163	Uranium extraction using a magnetic CoFe ₂ O ₄ –graphene nanocomposite: kinetics and thermodynamics studies. New Journal of Chemistry, 2015, 39, 2832-2838.	2.8	36
164	Magnesium carbonate basic coating on cotton cloth as a novel adsorbent for the removal of uranium. RSC Advances, 2015, 5, 23144-23151.	3.6	9
165	Preparation of magnetic core–shell iron oxide@silica@nickel-ethylene glycol microspheres for highly efficient sorption of uranium(vi). Dalton Transactions, 2015, 44, 6909-6917.	3.3	32
166	Composite of hierarchical interpenetrating 3D hollow carbon skeleton from lotus pollen and hexagonal MnO ₂ nanosheets for high-performance supercapacitors. Journal of Materials Chemistry A, 2015, 3, 9754-9762.	10.3	45
167	Fabrication of urchin-like NiCo ₂ (CO ₃) _{1.5} (OH) ₃ @NiCo ₂ S ₄ on Ni foam by an ion-exchange route and application to asymmetrical supercapacitors. Journal of Materials Chemistry A. 2015. 3. 13308-13316.	10.3	101
168	Synthesis, characterization and enhanced gas sensing performance of porous ZnCo ₂ O ₄ nano/microspheres. Nanoscale, 2015, 7, 19714-19721.	5.6	72
169	Facile synthesis of mesoporous ZnO/Co3O4 microspheres with enhanced gas-sensing for ethanol. Sensors and Actuators B: Chemical, 2015, 221, 1492-1498.	7.8	64
170	Preparation of magnetic calcium silicate hydrate for the efficient removal of uranium from aqueous systems. RSC Advances, 2015, 5, 5904-5912.	3.6	25
171	The synthesis of a manganese dioxide–iron oxide–graphene magnetic nanocomposite for enhanced uranium(<scp>vi</scp>) removal. New Journal of Chemistry, 2015, 39, 868-876.	2.8	84
172	Enhanced adsorption of uranium (VI) using a three-dimensional layered double hydroxide/graphene hybrid material. Chemical Engineering Journal, 2015, 259, 752-760.	12.7	229
173	Hierarchical NiCo ₂ O ₄ @NiO core–shell hetero-structured nanowire arrays on carbon cloth for a high-performance flexible all-solid-state electrochemical capacitor. Journal of Materials Chemistry A, 2014, 2, 1448-1457.	10.3	154
174	Manganese dioxide core–shell nanowires in situ grown on carbon spheres for supercapacitor application. CrystEngComm, 2014, 16, 4016.	2.6	31
175	Facile growth of hollow porous NiO microspheres assembled from nanosheet building blocks and their high performance as a supercapacitor electrode. CrystEngComm, 2014, 16, 10389-10394.	2.6	51
176	Self-assembly of ZnO nanoparticles into hollow microspheres via a facile solvothermal route and their application as gas sensor. CrystEngComm, 2013, 15, 7243.	2.6	71
177	Self-assembly of ZnO nanosheets into flower-like architectures and their gas sensing properties. Materials Letters, 2013, 112, 23-25.	2.6	44
178	Hierarchically porous MgAl mixed metal oxide synthesized by sudden decomposition of MgAl layered double hydroxide gel. New Journal of Chemistry, 2013, 37, 2128.	2.8	4
179	Mesoscopic titania solar cells with the tris(1,10-phenanthroline)cobalt redox shuttle: uniped versus biped organic dyes. Energy and Environmental Science, 2011, 4, 3021.	30.8	98